ACS Chemical Neuroscience 7.8 (2016): 1157–1165

DOI: 10.1021/acschemneuro.6b00122

TITLE

N-benzylpiperidine derivatives as α7 nicotinic receptor antagonists

AUTHOR LIST

Manuel Criado,* José Mulet, Francisco Sala, Salvador Sala, Inés Colmena, Luis Gandía, Oscar M. Bautista-Aguilera, Abdelouahid Samadi, Mourad Chioua, José Marco-Contelles

ABSTRACT

A series of multi-target directed propargylamines, as well as other differently susbstituted piperidines have been screened as potential modulators of neuronal nicotinic acetylcholine receptors (nAChRs). Most of them showed antagonist actions on α7 nAChRs. Especially, compounds **13**, **26** and **38** displayed sub-micromolar IC_{50} values on homomeric α7 nAChRs whereas they were less effective on heteromeric α3β4 and α4β2 nAChRs (up to 20-fold higher IC_{50} values in the case of **13**). Antagonism was concentration dependent and non-competitive, suggesting that these compounds behave as negative allosteric modulators of nAChRs. Upon the study of a series of less complex derivatives, the *N*-benzylpiperidine motif, common to these compounds, was found to be the main pharmacophoric group. Thus, 2-(1-benzylpiperidin-4-yl)-ethylamine (**48**) showed an inhibitory potency comparable to the one of the previous compounds and also a clear preference for α7 nAChRs. In a neuroblastoma cell line, representative compounds **13** and **48** also inhibited, in a concentration-dependent manner, cytosolic Ca^{2+} signals mediated mainly by α7 nAChRs. Finally, these compounds, especially **38** and **13**, inhibited 5-HT_{3A} serotonin receptors whereas they had no effect on α1 glycine receptors.

KEYWORDS: *Nicotinic receptors, Piperidine derivatives, α7, Ionic currents, blockers.*

INTRODUCTION

Neuronal nicotinic acetylcholine receptors (nAChRs) are ion channels that modulate fast synaptic transmission in nerve cells and are widely found in both the peripheral and central nervous systems. They are composed of five subunits assembled around the ion pore. Twelve subunits (α2-α10 and β2-β4) have been identified and cloned. Heteromeric or homomeric assembly of subunits result in the expression of functional nAChRs whose pharmacological and electrophysiological properties depend on their subunit composition[1]. Homomeric α7 nAChRs have received much attention, given their characteristic features, different of other neuronal nAChRs, such as rapid channel activation and inactivation and high Ca^{2+} permeability.[2] The latter property suggests the involvement of α7 nAChRs in processes beyond their channel activity.[3] Since α7 nAChRs appear to play an important role in central and peripheral diseases that involve, among others, cognition disorders,[4-6] schizophrenia,[7] pain[8] and inflammation,[9] considerable effort has been dedicated to develop therapeutic agents that target this receptor subtype.[10]

In the last years, some of us have reported a number of multi-target directed propargylamines (MTDP) able to bind simultaneously the cholinesterase and monoamine oxidase enzymes as a promising therapeutic strategy for the development of new drugs for Alzheimer's disease (AD).[11] Particularly attractive has resulted MTDP **ASS234**, a hybrid molecule resulting from the juxtaposition of donepezil (DNP) (Aricept®), a cholinesterase inhibitor currently prescribed for AD patients, and MTDP **PF9601N (1)** (Figure 1), a potent and selective MAO B inhibitor previously developed in our laboratory.[12, 13] At present, **ASS234** is our most advanced lead-compound for the potential treatment of AD.[14-16]

Based on these precedents, and in order to potentiate the polyphamarcology of hybrid **ASS234** for AD, we focused on its potential ability to modulate nAChRs. In fact, the capacity

of diversely substituted piperidines to act as α7 nAChR antagonists[17] and the presence of the *N*-benzylpiperidine motif in compound **ASS234**, set up the rational basis to start this project. As a result, we have explored a number of MTDPs from our stock library and current research projects, as well as other differently susbstituted piperidines as potential modulators of nAChRs. This effort enabled us to identify several hybrid molecules able to strongly inhibit α7 nAChRs, as well as detect the *N*-benzylpiperidine structural motif, present in almost all the compounds studied, as the main pharmacophoric group responsible for the inhibitory activity.

RESULTS AND DISCUSSION

Propargylamine ASS234 inhibits α7 nAChRs. Compound **ASS234** was evaluated as modulator of α7 nAChRs expressed in *Xenopus* oocytes. For this purpose, different concentrations of **ASS234** were co-applied with acetylcholine (ACh) (200 μM), and the resulting currents were compared to those induced by ACh alone (Figure 2A). In the presence of **ASS234** a substantial decrease was observed in the ionic currents. Their decay, however, was similar to control currents, so that changes in kinetics were not apparent (Figure 2A). The inhibitory effect of **ASS234** is dose dependent. Figure 2B shows concentration-response relationships of the effect of **ASS234** on peak currents of α7 nAChRs. IC_{50} value was close to 2 μM. Concentration-response relationships of ACh for α7 nAChRs (Figure 2C) were generated. In all cases there is a reduction of Imax (of about 70%) in the presence of **ASS234** suggesting a noncompetitive mechanism of action of this compound on α7 nAChRs. Furthermore, we observed a slight right shift of the apparent EC_{50} that increased by a factor of about 2. Finally, compound **ASS234** was also evaluated for its activity at α4β2 and α3β4 nAChRs expressed in *Xenopus* oocytes, as these two receptor subtypes constitute typical representatives of central and peripheral heteromeric receptors, respectively. While **ASS234** was able to inhibit the currents induced by ACh at these receptor subtypes, the effect was less prominent than in α7 receptors (Figure 2D). Thus, in the presence of 10 μM **ASS234**, 30.5 and 48% of the ACh-evoked current was inhibited in α3β4 and α4β2 nAChRs, respectively, whereas in α7 nAChRs, a current inhibition of 94.5% was observed. Therefore, **ASS234** is highly although not totally selective towards α7 nAChRs.

Screening of a library of structurally related compounds. Given the results obtained with **ASS234** we decided to explore a library of structurally related compounds **1-41** (Figures 1, 4 and 1S-8S, see **Supporting Information**) that had been designed, synthesized

and biologically evaluated in the context of our current program targeted to discover new molecules for AD.[12, 18-22]

As in the case of **ASS234**, each compound was individually tested by co-application with ACh to α7 nAChRs. As shown in Figure 3, a varied degree of inhibitory responses of ACh-induced currents was observed, whereas no significant potentiation was exerted by any of the tested compounds. A more detailed comparison of the most potent inhibitors and DNP, as a reference (see Figure 4 for chemical structures), is shown in Table 1. At 1 μM the most effective inhibitors were compounds **13**, **26** and **38**, whereas related compounds **11**, **22**, **37** and **39** induced weaker responses, and DNP did not affect the current. By contrast, at 10 μM all compounds, with the exception of DNP, were equally effective, inhibiting the ACh-induced current almost totally. DNP only inhibited half of the current at this concentration (Table 1).

Table 1. Effect of two different concentrations of DNP and the most potent inhibitors on ACh-evoked currents in α7 nAChRs.[a]

Compound	Normalized current	
	1 μM	**10 μM**
DNP	97±6.6	50.3±2.8
11	57.3±9.4	3±3
13	16.3±2.8	1.5±0.5
22	70±6.4	1
26	29.7±5.8	1
37	73±0.6	2.7±0.3
38	30.3±2.2	0
39	48.3±0.9	0.7±0.3

[a]Mean (± S.E.) currents of α7 nAChRs elicited by 200 μM ACh in the presence of the indicated concentrations of the different compounds. The currents are normalized to control values (100%) observed with only ACh.

Figure 5 features a more comprehensive study of DNP and the most potent inhibitors (**13**, **26** and **38**). Concentration-response relationships (Figure 5A) showed that compound **13** was almost 2-fold more potent than compounds **26** and **38** and about 30-fold more potent than DNP in blocking α7 nAChRs responses elicited by 200 μM ACh. Concentration-response relationships for ACh were slightly displaced to the right in the presence of all compounds (Figure 5B). Thus, EC_{50} for ACh was 202 μM in control conditions and 360, 424, 563 and 676 μM in the presence of compounds **38**, **13**, DNP, and **26**, respectively. Although these data do not rule out totally a competitive mechanism, they strongly suggest that these compounds behave as negative allosteric modulators of the α7 nAChRs.

Compounds **13**, **26**, **38** and DNP were also evaluated for its activity at α3β4 and α4β2 nAChRs (Figure 6A). The inhibiting action was less prominent in all cases, especially on α4β2 nAChRs. Thus, in the presence of 10 μM **13**, only 59% of the ACh-evoked current was inhibited in α3β4 and α4β2 nAChRs. DNP and **26** were even less effective in their inhibition (about 36-12%) whereas **38** showed more inhibition of α3β4 (66%) than of α4β2 currents (42%). At this concentration compounds **13**, **26** and **38** inhibited totally α7 currents (Table 1) In order to compare IC_{50} values in the three receptor subtypes, we determined concentration-response relationships of **13** for α3β4 and α4β2 nAChRs (Figure 6B). Thus, the IC_{50} values for α3β4 and α4β2 nAChRs were 7.2 and 6 μM, respectively, about 20-fold higher than in the case of α7 nAChRs. Therefore, and as previously observed with **ASS234**, the compounds are clearly more potent on α7 nAChRs.

Derivatives of *N*-benzylpiperidine act as inhibitors of α7 nAChRs. Despite their structural heterogeneity, all compounds from the previous screening that showed significant inhibitory activity, had in common the *N*-benzylpiperidine motif. Therefore, it would be of

interest to clear the role of this functional and structural motif as potential pharmacophoric group responsible for the observed biological activity.

For this purpose, we explored the activity of less bulky *N*-benzylpiperidine derivatives, such as chlorides **42**,[23] **43**,[24] alcohols **44**,[25] **45**,[26] and amines **46**,[25] **47**,[27] **48**,[28] **49**,[29] and **50**[30] (Figure 7) on α7 nAChRs. The effect of 1 and 10 μM *N*-benzylpiperidines on the magnitude of α7 nAChR peak currents elicited by ACh is shown in Figure 8. The most effective *N*-benzylpiperidines were amines **47-50**, which exhibited almost complete inhibition of α7 currents at 10 μM. These compounds were selected for a more detailed study of concentration-response relationships (Figure 9). Compound **48** was the most potent inhibitor (IC_{50} 0.58 μM), with compounds **49** and **50** having intermediate potencies (IC_{50} 1.4 and 1 μM, respectively) and compound **47** being the less potent (IC_{50} 2.2 μM). Therefore, a separation of two carbon atoms between the piperidine and the amino group seems optimal for the antagonist activity of these derivatives. Concentration-response relationships for ACh were slightly displaced to the right in the presence of all compounds (Figure 9B). Thus, EC_{50} for ACh was 207 μM in control conditions and 458, 312, 369 and 277 μM in the presence of compounds **47**, **48**, **49**, and **50**, respectively, suggesting that these compounds also behave as negative allosteric modulators of the α7 nAChRs. The inhibitory potency of compound **48** is comparable to the one of compounds **26** and **38**, and only two-fold lower that of compound **13**.. In addition, and as it was observed with the latter compounds, **48** was less effective on α3β4 and α4β2 nAChRs. Thus, at 10 μM **48**, which totally inhibited α7 currents, 68 % inhibition was observed in α3β4 as well as in α4β2 nAChRs (not shown).

Therefore, it appears that the *N*-benzylpiperidine moiety of these compounds is critical for their inhibitory activity, and that additional components such as the voluminous pyridinepropargylamine, 5-*O*-alkylindolomethylamine and indoloallylamine or much smaller

as ethylamine, present in compounds **13**, **26**, **38** and **48**, respectively, contribute to enhance the inhibitory activity.

Inhibition of cytosolic Ca^{2+} signals in a neuroblastoma cell line by compounds 13 and 48. To explore the action of these compounds in a different context, we examined their effect on the cytosolic Ca^{2+} signals ($[Ca^{2+}]_c$) elicited by application of 200 μM ACh in SH-SY5Y neuroblastoma cells that express α7 and α3* nAChRs. [31] Compound **13** was chosen because it showed the largest potency in previous experiments, whereas compound **48**, although having about the half of potency, also contained the *N*-benzylpiperidine motif but with much reduced molecular complexity. Figure 10A shows representative experiments carried out in SH-SY5Y cells in the absence (left panel) and in the presence of increasing concentrations of compounds **13** (central panel) and **48** (right panel). Application of only ACh elicited a sharp increase in $[Ca^{2+}]_c$ that reached a plateau and then tended to slowly decline along the 50 s of the recording (left panel). A significant portion of this cholinergic signal seems to be mediated by α7 nAChRs, since it was increased about 2-fold in the presence of the specific α7 allosteric potentiator PNU120598[32] (left panel). Preincubation of the cells with different concentrations of compounds **13** (center panel) and **48** (left panel) for 10 min induced a concentration-dependent decrease of the ACh-induced $[Ca^{2+}]_c$ increase. Figure 10B shows concentration-response curves obtained by using this type of protocol in cells from three different cell cultures and five different concentrations of the compounds (0.3, 1, 3, 10, and 30 μM). At the maximal concentrations of both compounds used, a 20% of the $[Ca^{2+}]_c$ signal remained unblocked, probably reflecting their lower effect on the non-α7 nAChRs, which are present in these cells.[31] The IC_{50} was calculated as 3.7 μM for compound **13** and 1.7 μM for compound **48**. Thus, in this experimental setting, compound **48** was about two-fold more potent than compound **13**.

Action on other ligand-gated ion channels. Finally, we explored the effect of representative compounds (DNP, **ASS234**, **13**, **26**, **38** and **48**) on glycine- and serotonin-activated receptors expressed in *Xenopus* oocytes.

At a 10 μM concentration no effect of any of these compounds was observed on homomeric α1 glycine receptors activated by 100 μM glycine (not shown). However, and except DNP, all of them inhibited 5-HT_{3A} serotonin receptors at different extent (Figure 11A). The most potent compounds were **38** and **13** (91 and 84 % inhibition, respectively), followed by **26**, **ASS234** (which showed a similar inhibition on α3β4 nAChRs, see Figure 2) and **48**. Compounds **13** and **38** were selected for a more detailed study of concentration-response relationships (Figure 11B). Compound **13** was the most potent inhibitor (IC_{50} 1.4 μM). This potency is intermediate between the observed with α7 nAChRs (0.32 μM) and the ones for α4β2 (6 μM) and α3β4 nAChRs (7.2 μM). Similarly, compound **38** was about 4-fold less potent with 5-HT_{3A} receptors (IC_{50} 2.1 μM) than with α7 nAChRs (IC_{50} 0.56 μM).

CONCLUSION

In this study we have investigated the effect of different MTDPs on the function of nAChRs. We have found that MTDPs inhibit the peak current of nAChRs without modifying the macroscopic kinetics of the currents. The blocking effect of MTDPs on nAChRs is reversible and seems to be non-competitive. All the MTDPs analyzed in detail (**ASS234** and compounds **13**, **26** and **38**) appears to be highly selective for α7 nAChRs, although they can also inhibit to a lesser extent α3β4 and α4β2 nAChRs, as well as 5-HT_{3A} serotonin receptors. These compounds have been considered potentially interesting for the treatment of AD, because their inhibitory actions on cholinesterase and monoamine oxidase enzymes.[11, 19, 21, 22] However, they might have a negative influence in this treatment, if we consider that activation, instead of inhibition, of neuronal nAChRs, and especially of the α7 subtype, is actually explored as a possibility of therapeutic intervention in AD.[33] Nevertheless, the mechanism of action of α7 nAChRs on AD appears to be very complex,[34] since both neuroprotection[35] and neurotoxicity[36] may be influenced by α7 nAChR activity. And, given the multifactorial nature of AD, the same might happen at the level of compounds used at present in its treatment. Thus, the frequently used galantamine and donepezil are both cholinesterase inhibitors, but the former can also act as positive allosteric modulator of neuronal nAChRs,[37] whereas we have shown that donepezil behaves as a weak negative allosteric modulator (Figure 5). Also, compound **ASS234** behaves as a cholinesterase inhibitor[14] as well as a noncompetitive antagonist of neuronal nAChRs (Figure 2) but, in addition, inhibits Aβ aggregation and protects from Aβ-induced apoptosis in vitro,[15] affecting in this way different processes involved in AD pathogenesis. Therefore, it is evident that the evaluation of a compound for its use in AD treatment must take into account many and rather diverse parameters.

All the studied donepezil derivatives bear in common the *N*-benzylpiperidine structural motif. Recently, α7 antagonists containing this motif have been described (the so-called compounds 7, 7i and 8),[17] although they differ at the rest of the molecule and are about 10-20-fold less potent acting on human α7 nAChRs expressed in *Xenopus* oocytes, thus confirming the importance of the non-piperidine component on the antagonistic properties. In fact, our study of less bulky derivatives showed that the ethylamine one (compound **48**) was as potent as the larger ones (Figures 7-10). To our knowledge no other biological activity has been described for this molecule, which is only mentioned in a virtual search for trypanothione reductase inhibitors but with no positive result.[38] Therefore, compound **48** could be a good starting point for further development of either positive or negative allosteric modulators of α7 nAChRs with therapeutic potential in AD as well as in others diseases in which inhibition of this receptor subtype might play an important role. [39]

EXPERIMENTAL SECTION

Synthesis. All compounds described here have been prepared as indicated in the corresponding references.

7-(3-(1-Benzylpiperidin-4-yl)propoxy)-3-phenyl-2H-chromen-2-one ASS352 (9). To a solution of 7-hydroxy-3-phenyl-2*H*-chromen-2-one[40] (0.1 g, 0.42 mmol) and 1-benzyl-4-(3-chloropropyl)piperidine[14] (0.106 g, 0.42 mmol) in DMF (2 mL), NaH (16.8 mg, 1.73 mmol, 60% /mineral) was added. The reaction mixture was stirred at room temperature overnight. After complete reaction (tlc analysis), the reaction was concentrated, diluted with water, and extracted with CH_2Cl_2. The organic phase was washed with brine, dried ($MgSO_4$), and evaporated at reduced pressure. The crude product was purified by flash chromatography (CH_2Cl_2/AcOEt, 10:1 to 5/1, v/v) to give compound **ASS352.** (181.4 mg, 95%) as a white solid: R*f* = 0.3 (hexane/EtOAc, 1/1); amorphousn solis; IR (KBr) ν 3430, 2936, 2920, 1708, 1621, 1605, 1336, 1272, 1180, 1125 cm^{-1}; ^1H NMR (500 MHz, $CDCl_3$) δ 7.76 (s, CH-4), 7.71-7.67 (m, 2CH), 7.46-7.36 (m, 4H, Ph), 7.34-7.28 (m, 4H, Ph), 7.28-7.21 (CH, Ph), 6.86-6.83 (m, 2CH, CH-6+CH-8), 4.02 (t, *J*= 6.5 Hz, 2H, -*CH*$_2$-O-), 3.51 (s, 2H, Ph*CH*$_2$), 2.90 (d, *J*= 10.6 Hz, 1H, CH_2, piperidine), 1.96 (t, *J*= 9.7 Hz, 2H, CH_2, piperidine), 1.87-1.79 [m, 2H, -*CH*$_2$-(CH_2O)], 1.70 (d, *J*= 9.1 Hz, 2H, CH_2, piperidine), 1.43-1.40 [m, 2H, -*CH*$_2$-$(CH_2)_2O$-], 1.31 (bs, 3H, CH+CH_2, piperidine); ^{13}C NMR (125 MHz, $CDCl_3$) δ 162.1 (C7), 160.9 (C2), 155.3 (C8a), 140.0 (CH-4), 138.5 (C, Ph), 135.0 (C, Ph), 129.2 (2CH, Ph), 128.7 (C5), 128.4 (2CH, Ph), 128.3 (2CH, Ph), 128.1 (2CH, Ph), 126.9 (CH, Ph), 113.1 (C6), 113.2 (C4a), 100.8 (C8), 68.8 (CH_2O), 63.4 (Ph*CH*$_2$), 53.8 (2CH_2, piperidine), 35.6 (CH, piperidine), 32.8 [-*CH*$_2$-$(CH_2)_2O$], 32.3 (2CH_2, piperidine), 26.3 [-*CH*$_2$-CH_2O]; MS (EI) *m/z* (%): 454.57 $[M+H]^+$, 476.56 $[M+Na]^+$. HRMS: Calculated for $C_{30}H_{31}NO_3$ 454.2377 $[M+H]^+$. Found 454.2363. Anal. Calcd. for $C_{30}H_{31}NO_3$: C, 79.44; H, 6.89; N, 3.09. Found: C, 79.67; H, 6.78; N, 3.22.

Oocyte expression. All cDNAs were cloned in derivatives of the pSP64T vector[41] containing part of the pBluescript polylinker. Capped mRNA was synthesized in vitro using SP6 RNA polymerase, the mMESSAGE-mMACHINE kit (ThermoFisher, Madrid, Spain) and the same pSP64T derivatives mentioned above. Defoliculated *Xenopus laevis* oocytes

were injected with 5 ng of each subunit cRNA in 50 nL of sterile water. All experiments were performed within 2-3 days after cRNA injection.

Electrophysiological recordings. Two electrode voltage-clamp electrophysiological recordings in *Xenopus* oocytes were carried out as previously described.[42] The extracellular solution contained (in mM): NaCl 82.5, KCl 2.5, $BaCl_2$ 2.5, $MgCl_2$ 1.0 and HEPES 5 (pH 7.4) The replacement of calcium by barium in this solution diminishes the activation of calcium-activated chloride currents. The velocity of application of agonists through a tube located very close to the oocyte was 18-22 mL/min. The solution exchange rate followed an exponential time course with a time constant of 90 ms.[43] Unless otherwise specified, compounds were pre-applied in the bath for 2 minutes and then co-applied with ACh through a pipette held very close to the oocyte for fast application and functional responses were estimated as the peak ionic current evoked by 4 s application of 200 μM ACh at -80 mV. All experiments were performed at 22ºC. Current records were measured with Clampfit 10.0 (MDS Analytical Technologies, Sunnyvale, CA, USA).

Data analysis. Normalized peak currents were obtained by dividing the maximum value of the current obtained in the presence of the compound by the maximum value of the current obtained in control conditions. Dose-response curves for the peak current obtained with ACh were fitted to the Hill equation:

Normalized current = $I_{max} / (1 + (EC_{50} / [ACh])^{nH})$, and dose-response inhibition curves were fitted to the modified Hill equation:

Normalized current = $1 / (1+ ([compound] / IC_{50})^{nH})$.

Data are expressed as mean ± SEM.

SH-SY5Y cell culture. SH-SY5Y neuroblastoma cells were maintained in DMEM/Ham's F-12 (1:1) media supplemented with 10% foetal calf serum, 2 mM glutamine, 50 U/mL penicillin, and 50 μg/mL streptomycin (all products were purchased from Sigma,

Madrid, Spain), and were split every 3-4 d. For measurements of $[Ca^{2+}]_c$, cells were plated at a density of $2x10^5$ cells per well into 96-well plates. Cells were kept for 2 days at 37°C in a water-saturated incubator, with a 5% CO2/95% air atmosphere. Experiments were performed at room temperature (24±2°C).

Measurement of $[Ca^{2+}]_c$. Cells were loaded with Krebs-HEPES (in mM: 144 NaCl, 5.9 KCl, 1.2 $MgCl_2$, 2 $CaCl_2$, 11 D-glucose, 10 HEPES, pH 7.4) containing 10 μM fluo-4 AM for 45 min at 37°C in the dark. After this incubation period, cells were washed twice with Krebs-HEPES at room temperature in the dark. Changes in fluorescence (excitation 485 nm, emission 520 nm) were measured using a fluorescent plate reader (Fluostar, BMG Labtechnologies). Basal levels of fluorescence were monitored before adding stimulation solution (200 μM ACh) by using an automatic dispenser. After stimulation, changes in fluorescence were measured for 50 seg. To normalize fluo-4 signals, responses from each well were calibrated by measuring maximum and minimum fluorescence values. At the end of each experiment, addition of 5% Triton X-100 (Fmax) was followed by addition of 1 M $MnCl_2$ (Fmin). Data were calculated as a percentage of Fmax - Fmin.

SUPPORTING INFORMATION

Chemical structure of additional compounds is available free of charge via the Internet at http://pubs.acs.org.

Abbreviations

ACh, acetylcholine; AD, Alzheimer's disease; DNP, donepezil; MTDP, propargylamine; nAChRs, neuronal nicotinic acetylcholine receptors.

Author Information.

Manuel Criado, Instituto de Neurociencias, Universidad Miguel Hernandez-CSIC, 03050-Sant Joan d'Alacant (Spain). E-mail: manuel.criado@umh.es

Acknowledgement.

This work was supported by grants SAF2011-22802 to S.S., SAF2012-33304 to J.M.-C., CSD2008-00005 (the Spanish Ion Channel Initiative-CONSOLIDER INGENIO 2010) to M.C. from the Spanish Ministry of Science and Innovation (Ministerio de Economía y Competitividad).

References

(1) Dineley, K.T., Pandya, A.A., and Yakel, J.L. (2015) Nicotinic ACh receptors as therapeutic targets in CNS disorders. *Trends Pharmacol. Sci. 36*, 96-108.

(2) Sinkus, M.L., Graw, S., Freedman, R., Ross, R.G., Lester, H.A., and Leonard, S. (2015) The human *CHRNA7* and *CHRFAM7A* genes: A review of the genetics, regulation and function. *Neuropharmacol*. *96*, 274-288.

(3) Egea, J., Buendia, I., Parada, E., Navarro, E., León, R., and Lopez, M.G. (2015) Anti-inflammatory role of microglial alpha7 nAChRs and its role in neuroprotection. *Biochem. Pharmacol. 97*, 463-472.

(4) Parri, H.R., Hernandez, C.M., and Dineley, K.T. (2011) Research update: Alpha7 nicotinic acetylcholine receptor mechanisms in Alzheimer's disease. *Biochem. Pharmacol. 82*, 931-942.

(5) Quik, M., Zhang, D., McGregor, M., and Bordia, T. (2015) Alpha7 nicotinic receptors as therapeutic targets for Parkinson's disease. *Biochem. Pharmacol. 97*, 399-407.

(6) Deutsch, S.I., Burket, J.A., Urbano, M.R., and Benson, A.D. (2015) The α7 nicotinic acetylcholine receptor: A mediator of pathogenesis and therapeutic target in autism spectrum disorders and Down syndrome. *Biochem. Pharmacol. 97*, 363-377.

(7) Young, J.W., and Geyer, M.A. (2013) Evaluating the role of the alpha-7 nicotinic acetylcholine receptor in the pathophysiology and treatment of schizophrenia. *Biochem. Pharmacol. 86*, 1122-1132.

(8) Umana, I.C., Daniele, C.A., and McGehee, D.S. (2013) Neuronal nicotinic receptors as analgesic targets: It's a winding road. *Biochem. Pharmacol. 86*, 1208-1214.

(9) Matteoli, G., and Boeckxstaens, G.E. (2013) The vagal innervation of the gut and immune homeostasis. *Gut 62*, 1214-1222.

(10) Mazurov, A.A., Speake, J. D. and Yohannes, D. (2011) Discovery and development of α7 nicotinic acetylcholine receptor modulators. *J. Med. Chem. 54*, 7943–7961.

(11) Bolea, I., Gella, A., and Unzeta, M. (2013) Propargylamine-derived multitarget-directed ligands: Fighting Alzheimer's disease with monoamine oxidase inhibitors. *J. Neural Transm. 120*, 893-902.

(12) Cruces, M. A., Elorriaga, C., and Fernández-Álvarez, E. (1991) Acetylenic and allenic derivatives of 2-(5-benzyloxyindolyl) and 2-(5-hydroxyindolyl) methylamines: synthesis and in vitro evaluation as monoamine oxidase inhibitors. *Eur. J. Med. Chem. 26*, 33-41.

(13) Pérez, V., Marco, J.L., Fernández-Álvarez, E., and Unzeta, M. (1999). Relevance of benzyloxy group in 2-indolyl methylamines in the selective MAO-B inhibition. *Br. J. Pharmacol. 12*, 869-876.

(14) Bolea, I., Juárez-Jiménez, J., de los Ríos, C., Chioua, M., Pouplana, R., Luque, F.J., Unzeta, M., Marco-Contelles, J., and Samadi, A. (2011) Synthesis, biological evaluation, and molecular modeling

of donepezil and N-[(5-(benzyloxy)-1-methyl-1H-indol-2-yl)methyl]-N- methylprop-2-yn-1-amine. hybrids as new multipotent cholinesterase/monoamine oxidase inhibitors for the treatment of Alzheimer's disease. *J. Med. Chem. 54*, 8251-8270

(15) Bolea, I., Gella, A., Monjas, L., Pérez, C., Rodríguez-Franco, M. I., Marco-Contelles, J., Samadi, A., and Unzeta, M. (2013) Multipotent, permeable drug ASS234 inhibits Aβ aggregation, possesses antioxidant properties and protects from Aβ-induced apoptosis in vitro. *Curr Alzheimer Res. 10*, 797-808.

(16) Esteban, G., Allan, J., Samadi, A., Mattevi, A., Unzeta, M., Marco-Contelles, J., Binda, C., and Ramsay, R.R. (2014) Kinetic and structural analysis of irreversible inhibition of human monoamine oxidases by ASS234, a multi-target compound designed for use in Alzheimer's disease. *Biochim. Biophys. Acta. 1844*, 1104-1110.

(17) Peng, Y., Zhang, Q., Snyder, G. L., Zhu, H., Yao, W., Tomesch, J., Papke, R. L., O'Callaghan, J.P., Welsh, W. J., and Wennogle, L. P. (2010) Discovery of novel α7 nicotinic receptor antagonists, *Bioorg. Med. Chem. Lett. 20*, 4825–4830.

(18) Cruces, M. A., Elorriaga, C., Fernández-Álvarez, E., and Nieto López, O. (1990) Acetylenic and allenic derivatives of 2-(5-methoxyindolyl)methylamine: synthesis and evaluation as selective inhibitors of the monoamine oxidases A and B. *Eur. J. Med. Chem. 25*, 257-265.

(19) Bautista-Aguilera, O. M., Samadi, A., Chioua, M., Nikolic, K., Filipic, S., Agbaba, D., Soriano, E., de Andres, L., Rodríguez-Franco, M. I., Alcaro, S., Ramsay, R. R., Ortuso, F., Yañez, M., and Marco-Contelles, J. (2014) N- Methyl-N-((1-methyl-5-(3-(1-(2-methylbenzyl)piperidin-4-yl) propoxy)-1H-indol-2-yl)methyl)prop-2-yn-1-amine, a New Cholinesterase and Monoamine Oxidase Dual Inhibitor. *J. Med. Chem. 57*, 10455-10463.

(20) Cruces, M. A., Elorriaga, C., Fernández Álvarez, E., López Chico, M. T., Nieto, and López, O. (1988) Acetylenic and allenic derivatives of 2-(1-methylindolyl)methylamine as selective inhibitors of monoamine oxidases A and B. *Farmaco 43*, 567-573.

(21) Bautista-Aguilera, O. M., Esteban, G., Bolea, I., Nikolic, K., Agbaba, D., Moraleda, I., Iriepa, I., Samadi, A., Soriano, E., Unzeta, M., and Marco-Contelles, J. (2014) Design, synthesis, pharmacological evaluation, QSAR analysis, molecular modeling and ADMET of novel donepezil-indolyl hybrids as multipotent cholinesterase/monoamine oxidase inhibitors for the potential treatment of Alzheimer's disease. *Eur. J. Med. Chem. 75*, 82-95.

(22) Bautista-Aguilera, O. M., Esteban, G., Chioua, M., Nikolic, K., Agbaba, D., Moraleda, I., Iriepa, I., Soriano, E., Samadi, A., Unzeta, M., and Marco-Contelles, J. (2014) Multipotent cholinesterase/monoamine oxidase inhibitors for the treatment of alzheimer's disease: design, synthesis, biological/biochemical evaluation, admet, molecular modeling and qsar analysis of novel donepezil-pyridyl hybrids. *Drug Design, Development and Therapy 8*, 1893-1910.

(23) Popp, F. D., and Watts, R. F. (1978) The synthesis and ring opening of N-substituted-2-oxa-6-azaspiro[2.5]octanes. *J. Heterocyclic Chem. 15*, 675-676.

(24) Sugimoto, H., Tsuchiya, Y., Sugumi, H., Higurashi, K., Karibe, N., Iimura, Y., Sasaki, A., Araki, S., Yamanishi, Y., and Yamatsu, K. (1992) Synthesis and structure-activity relationships of acetylcholinesterase inhibitors: 1-benzyl-4-(2-phthalimidoethyl)piperidine, and related derivatives. *J. Med. Chem. 35*, 4542-4548.

(25) Commercially available.

(26) Mandelli, G. R., Maiorana, S., Terni, P., Lamperti, G., Colibretti, M. L., and Imbimbo, B. P. (2000) Synthesis of new cardioselective M2 muscarinic receptor antagonists. *Chem. Pharm. Bull. 48*, 1611-1622.

(27) Contreras, J.M., Rival, Y. M., Chayer, S., Bourguignon, J.-J., and Wermuth, C. G. (1999) Aminopyridazines as acetylcholinesterase inhibitors. *J. Med. Chem. 42*, 730-741.

(28) New, J. S., and Yevich, J. P. (1983) Applications of lithium aluminum hydride in the synthesis of substituted ethyl- and propylamines. *Synthesis* 388-389.

(29) Samadi, A., Chioua, M., Bolea, I., de los Ríos, C., Iriepa, I., Moraleda, I., Bastida, A., Esteban, G., Unzeta, M., Gálvez, E., and Marco-Contelles, J. (2011) Synthesis, biological assessment and molecular modeling of new multipotent MAO and cholinesterase inhibitors as potential drugs for the treatment of Alzheimer's disease. *Eur. J. Med. Chem. 46*, 4665-4668.

(30) Samadi, A., Estrada, M., Pérez, C., Rodríguez-Franco, M. I., Iriepa, I., Moraleda, I., Chioua, M., and Marco-Contelles, J. (2012) Pyridonepezils, new dual AChE inhibitors as potential drugs for the treatment of Alzheimer's disease: Synthesis, biological assessment, and molecular modeling. *Eur. J. Med. Chem. 57*, 296-301.

(31) Lukas, R.J., Norman, S.A., and Lucero, L. (1993) Characterization of nicotinic acetylcholine receptors expressed by cells of the SH-SY5Y human neuroblastoma clonal line. *Mol. Cell. Neurosci. 4*, 1-12.

(32) Hurst, R.S., Hajos, M., Raggenbass, M., Wall, T.M., Higdon, N.R., Lawson, J.A., Rutherford-Root, K.L., Berkenpas, M.B., Hoffmann, W.E., Piotrowski, D.W., Groppi, V.E., Allaman, G., Ogier, R., Bertrand, S., Bertrand, D., and Arneric, S.P. (2005) A novel positive allosteric modulator of the alpha7 neuronal nicotinic acetylcholine receptor: in vitro and in vivo characterization. *J. Neurosci. 25,* 4396-4405.

(33) Vallés, A.S., Borroni, M.V., and Barrantes, F.J. (2014) Targeting brain α7 nicotinic acetylcholine receptors in Alzheimer's disease: rationale and current status. *CNS Drugs 28*, 975-987.

(34) Shen, J., and Wu, J. (2015) Nicotinic cholinergic mechanisms in Alzheimer's disease (2015) *Int. Rev. Neurobiol. 124*, 275-292.

(35) Hernandez, C. M., Kayed, R., Zheng, H., Sweatt, J. D., and Dineley, K. T. (2010) Loss of alpha7 nicotinic receptors enhances beta-amyloid oligomer accumulation, exacerbating early-stage cognitive decline and septohippocampal pathology in a mouse model of Alzheimer's disease. *J. Neurosci. 30*, 2442–2453.

(36) Dziewczapolski, G., Glogowski, C. M., Masliah, E., and Heinemann, S. F. (2009) Deletion of the alpha 7 nicotinic acetylcholine receptor gene improves cognitive deficits and synaptic pathology in a mouse model of Alzheimer's disease. *J. Neurosci.29*, 8805–8815.

(37) Samochocki, M., Hoffle, A., Fehrenbacher, A., Jostock, R., Ludwig, J.,Christner, C., Radina, M., Zerlin, M., Ullmer, C., Pereira, E.F., Lubbert, H., Albuquerque, E.X., and Maelicke, A. (2003) Galantamine is an allosterically potentiating ligand of neuronal nicotinic but not of muscarinic acetylcholine receptors. *J. Pharmacol. Exp. Ther. 305*, 1024–1036.

(38) Horvath, D. (1997) A virtual screening approach applied to the search for trypanothione reductase inhibitors (1997) *J. Med. Chem. 40,* 2412-2423.

(39) Paleari, L., Cesario, A., Fini, M., and Russo, P (2009) α7-Nicotinic receptor antagonists at the beginning of a clinical era for NSCLC and mesothelioma. *Drug. Discov Today 14*, 822-836.

(40) Olmedo, D., Sancho, R., Bedoya, L. M., López-Pérez, J. L., del Olmo, E., Muñoz, E., Alcami, J., Gupta, M. P., and San Feliciano, A. (2012) 3-Phenylcoumarins as inhibitors of HIV-1 replication, *Molecules 17*, 9245-9257

(41) Krieg, P. A. and Melton, D. A. (1984) Functional messenger RNAs are produced by SP6 in vitro transcription of cloned cDNAs. *Nucleic Acids Res. 12,* 7057-7070.

(42) Garcia-Guzman, M., Sala, F., Sala, S., Campos-Caro, A., and Criado, M. (1994) Role of two acetylcholine receptor subunit domains in homomer formation and intersubunit recognition, as revealed by alpha 3 and alpha 7 subunit chimeras. *Biochemistry 33,* 15198-15203.

(43) Sala, F., Mulet, J., Valor, L. M., Criado, M., and Sala, S. (2002) Effects of benzothiazepines on human neuronal nicotinic receptors expressed in Xenopus oocytes. *Br.J.Pharmacol. 136,* 183-192.

FIGURES

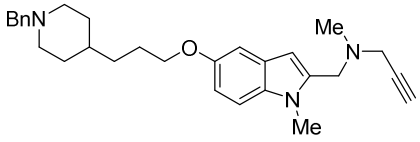

ASS234

IC_{50} (μM)			
*Ee*AChE	eqBuChE	rat MAO A	rat MAO B
0.35 ± 0.01	0.46 ± 0.06	0.0052 ± 0.0011	0.043 ± 0.008

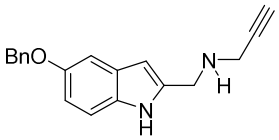

PF9601N (1)

Figure 1. Structure of compounds **ASS234** and **PF9601N** (**1**). IC_{50} values of **ASS234** for the inhibition of cholinesterase and monoamine oxidase enzymes are also indicated.

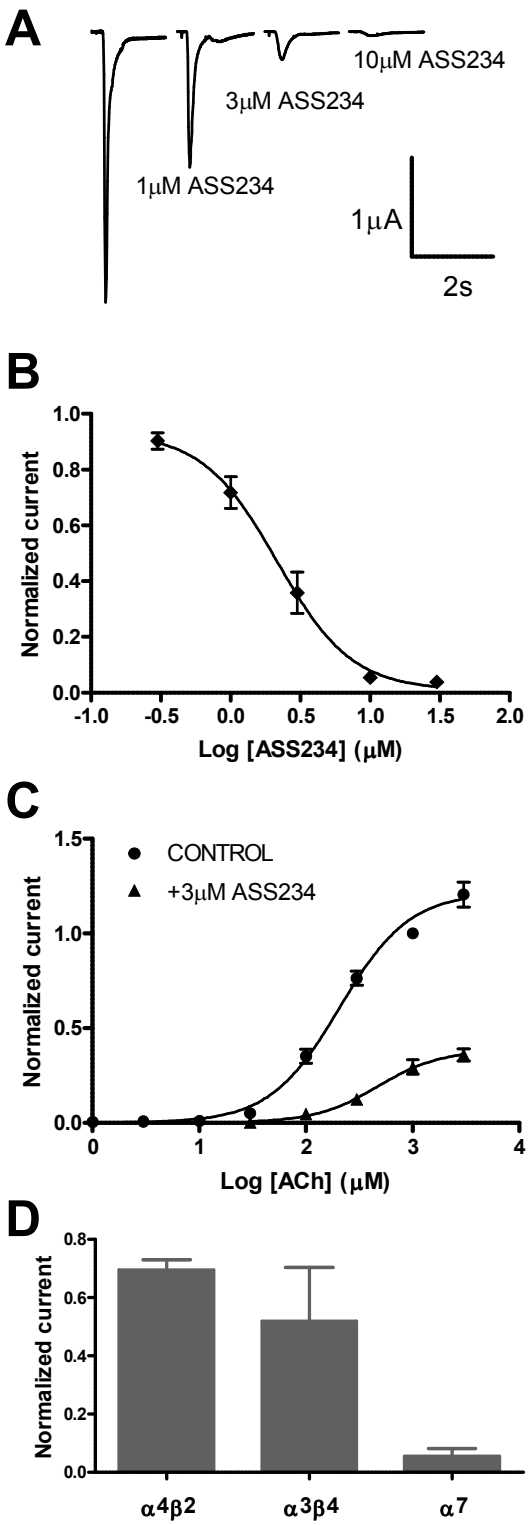
A
10μM ASS234
3μM ASS234
1μM ASS234
1μA
2s
B
Normalized current
1.0
0.8
0.6
0.4
0.2
0.0
-1.0
-0.5
0.0
0.5
1.0
1.5
2.0
Log [ASS234] (μM)
C
CONTROL
+3μM ASS234
Normalized current
1.5
1.0
0.5
0.0
0
1
2
3
4
Log [ACh] (μM)
D
Normalized current
0.8
0.6
0.4
0.2
0.0
α4β2
α3β4
α7

Figure 2. A) Representative ionic currents recorded in oocytes expressing human α7 nAChRs. Currents were evoked by 600 ms applications of ACh 200 μM in the absence (first trace) and in the presence (remaining traces) of 1, 3 and 10 μM of **ASS234**. All currents were recorded at a holding potential of -80 mV. B) Concentration-response relationship for the inhibiting effect of **ASS234** co-applied with ACh 200 μM. Continuous lines represent the fit to the Hill equation resulting in values of IC_{50} 2.2 ± 0.4 μM and nH 1.6 ± 0.4. C) ACh concentration-response relationship in the absence (circles) and in the presence (triangles) of 3 μM of **ASS234**, a concentration that was chosen because it is close to the IC_{50} value. All data were normalized to the response obtained by ACh 1 mM in control conditions. Continuous lines represent fits to Hill equations with the following parameters (I_{max}, EC_{50} in μM, nH) for ACh (1.22 ± 0.05, 207 ± 22, 1.3 ± 0.2) and ACh plus **ASS234** (0.38 ± 0.05, 472 ± 130, 1.5 ± 0.4). D) Normalized current of α7, α3β4 and α4β2 receptors elicited by ACh in the presence of 10 μM of **ASS234**. Control values of peak inward currents (in μA) were: α7, 1.32 ± 0.08; α4β2, 5.25 ± 0.42; α3β4, 11.62 ± 0.62.

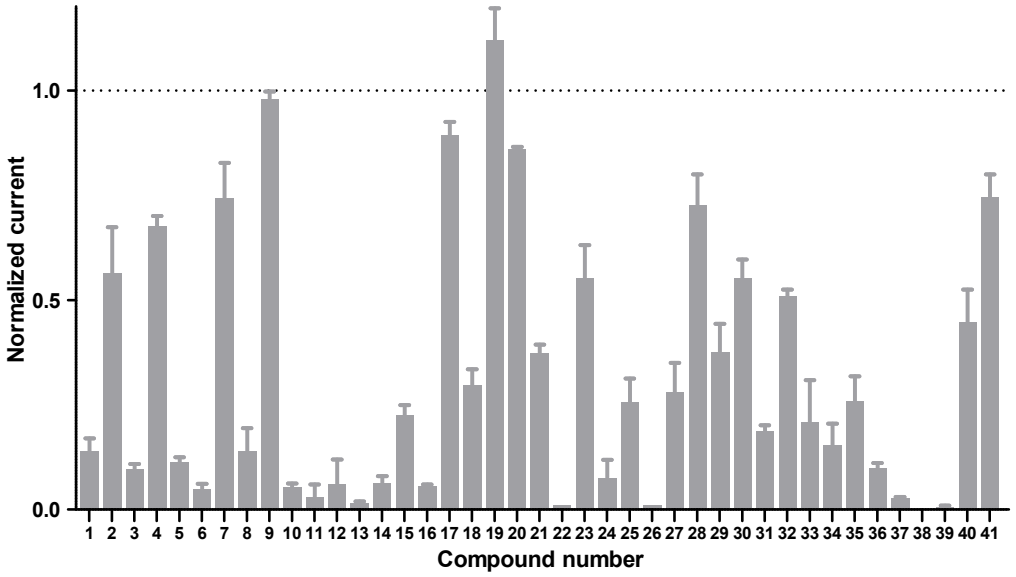

Figure 3. Normalized current of α7 nAChRs elicited by 200 μM ACh in the presence of 10 μM of compounds **1-41**. Control values of peak inward currents for α7 nAChRs were 1.22 ± 0.07 μA.

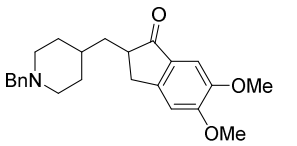

Donepezil

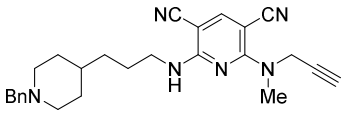

MV79 (11)

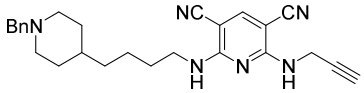

MBA115 (13)

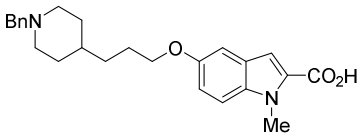

MBA73 (22)

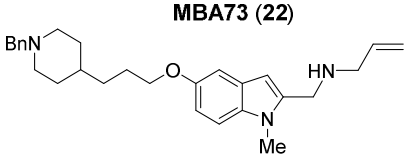

MBA98F2 (26)

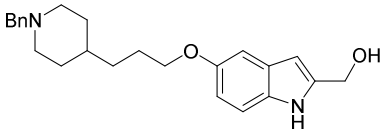

MBA294 (37)

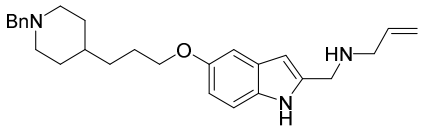

MBA319F2 (38)

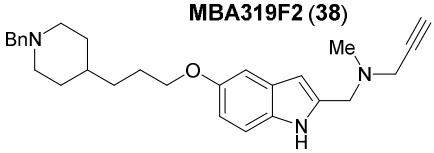

MBA314F1 (39)

Figure 4. Structure of DNP, and compounds **11**,[22] **13**,[22] **22**,[21] **26**,[21] **37**-**39**.[19]

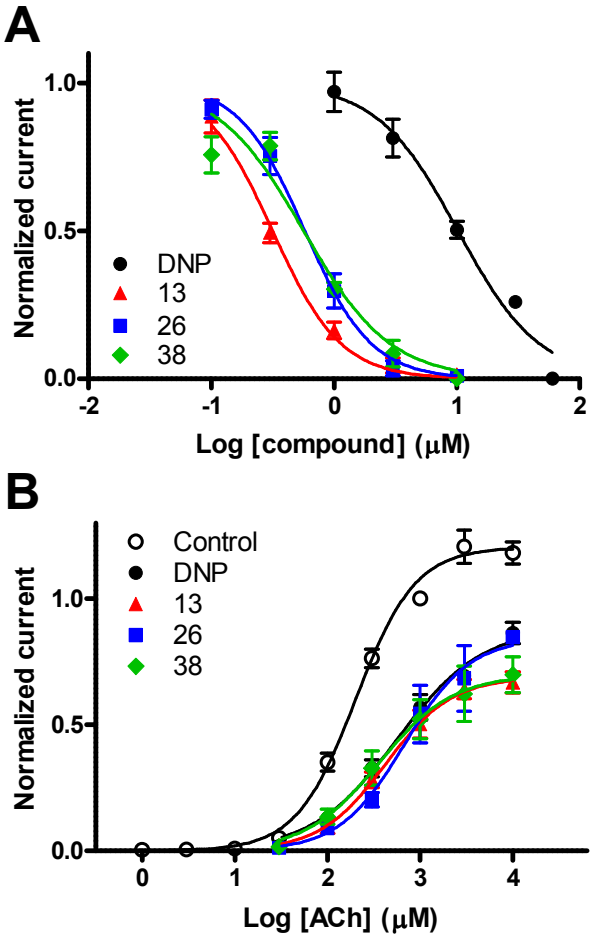

Figure 5. A) Dose-response curves of the inhibitory effect of compounds **13**, **26**, **38** and DNP on peak currents elicited by ACh 200 μM in α7 nAChRs. Curves are fits to the modified Hill equation with the following parameters (IC_{50} in μM, nH): **13** (0.32 ± 0.02, 1.6 ± 0.2), **26** (0.58 ± 0.05, 1.6 ± 0.2), **38** (0.56 ± 0.08, 1.2 ± 0.2) and DNP (10.2 ± 1.1, 1.3 ± 0.2). B) Dose-response curves of peak current elicited by ACh in control conditions or ACh in the presence of 0.3 μM **13**, 0.6 μM **26**, 0.6 μM **38** or 10 μM DNP. Data have been normalized to the peak current obtained in control conditions with 1 mM ACh. Lines are fits to the Hill equation with parameters (Imax, EC_{50} in μM, nH): control (1.2 ± 0.03, 202 ± 18.6, 1.4 ± 0.1), with **13** (0.69 ± 0.05, 424 ± 94.5, 1.2 ± 0.3), with **26** (0.84 ± 0.14, 676 ± 285, 1.2 ± 0.5), with **38** (0.7 ± 0.1, 360 ± 157, 1.1 ± 0.4) and with DNP (0.88 ± 0.08, 563 ± 148, 1 ± 0.2).

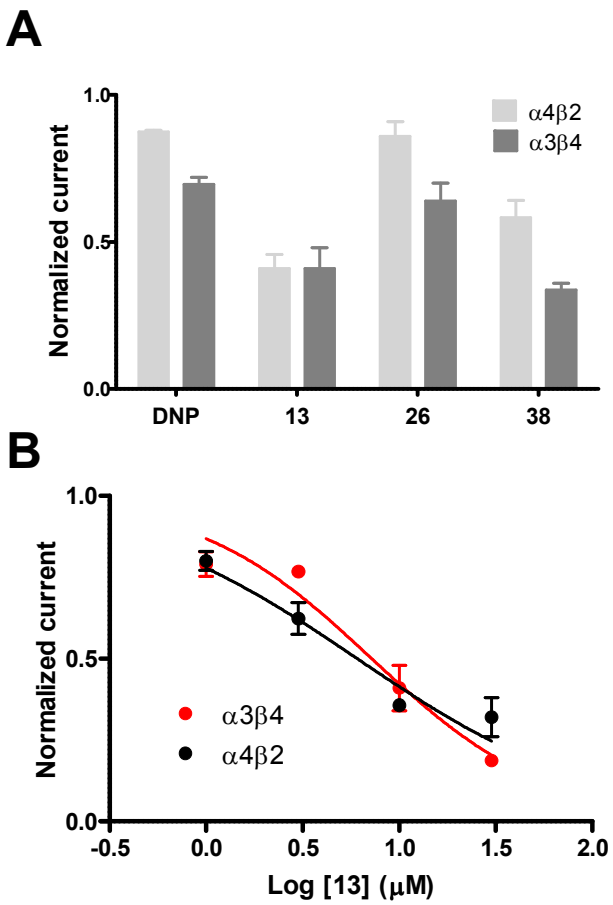

Figure 6. A) Normalized current of α3β4 and α4β2 nAChRs elicited 200 μM ACh in the presence of 10 μM of compounds **13, 26, 38** and DNP. Control values of peak inward currents (in μA) were: α4β2, 5.18 ± 0.29; α3β4, 10.57 ± 0.40. B) Dose-response curves of the inhibitory effect of **13** on peak currents elicited by 200 μM ACh in α3β4 and α4β2 nAChRs . Curves are fits to the modified Hill equation with the following parameters (IC_{50} in μM, nH): α3β4 (7.2 ± 1, 0.96 ± 0.1) and α4β2 (6 ± 0.9, 0.7 ± 0.1).

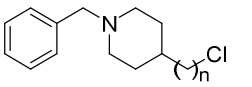

ASS8-HCl (**42** n= 1)

ASS276-HCl (**43** n= 2)

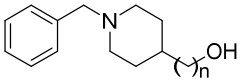

MV11 (**44** n= 1)

MBA384 (**45** n= 4)

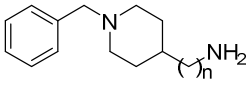

A7-34 (**46** n= 0)

MV18 (**47** n= 1)

MC-254 (**48** n= 2)

MC793b (**49** n= 3)

MC794F3 (**50** n= 4)

Figure 7. *N*-Benzylpiperidine derivatives **42-50**.

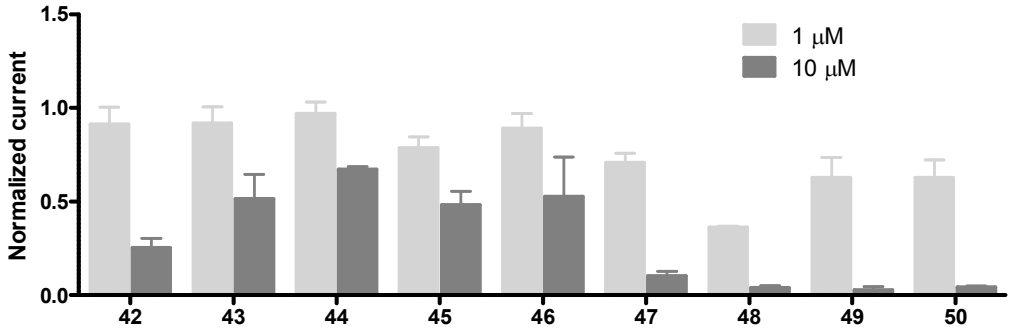

Figure 8. Normalized current of α7 nAChRs elicited by 200 μM ACh in the presence of 1 and 10 μM of the indicated compounds. Control values of peak inward currents for α7 nAChRs were 1.36 ± 0.1 μA.

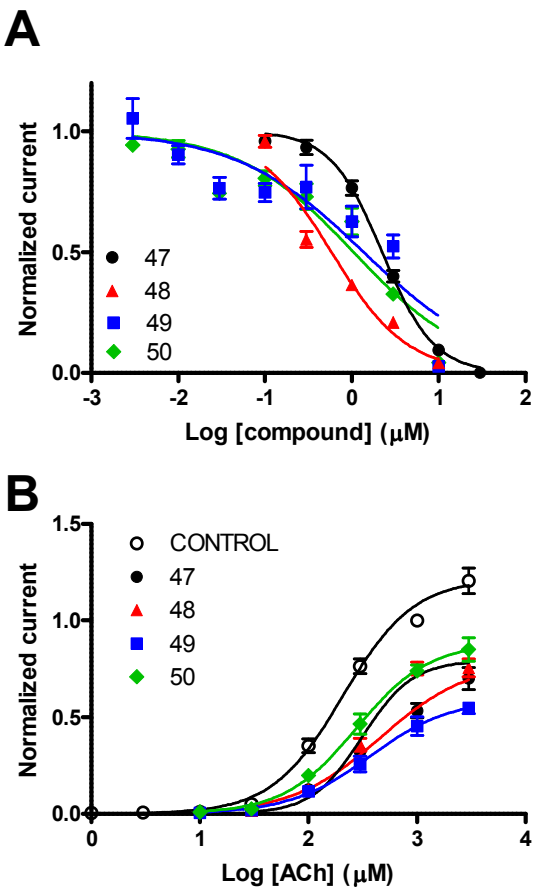

Figure 9. A) Dose-response curves of the inhibitory effect of compounds **47-50** on peak currents elicited by ACh 200 μM in α7 nAChRs. Curves are fits to the modified Hill equation with the following parameters (IC_{50} in μM, nH): **47** (2.2 ± 0.1, 1.5 ± 0.1), **48** (0.58 ± 0.07, 1 ± 0.1), **49** (1.4 ± 0.4, 0.6 ± 0.1) and **50** (1 ± 0.2, 0.7 ± 0.1). B) Dose-response curves of peak current elicited by ACh in control conditions or ACh in the presence of 2 μM **47**, 0.6 μM **48**, 2 μM **49** or 1 μM **50**. Data have been normalized to the peak current obtained in control conditions with 1 mM ACh. Lines are fits to the Hill equation with parameters (Imax, EC_{50} in μM, nH): control (1.22 ± 0.04, 207 ± 22.3, 1.3 ± 0.2), with **47** (0.79 ± 0.09, 458 ± 141, 1.1 ± 0.2), with **48** (0.79 ± 0.04, 312 ± 35, 1.9 ± 0.4), with **49** (0.59 ± 0.06, 369 ± 101, 1.2 ± 0.2) and with **50** (0.89 ± 0.05, 277 ± 45, 1.3 ± 0.2).

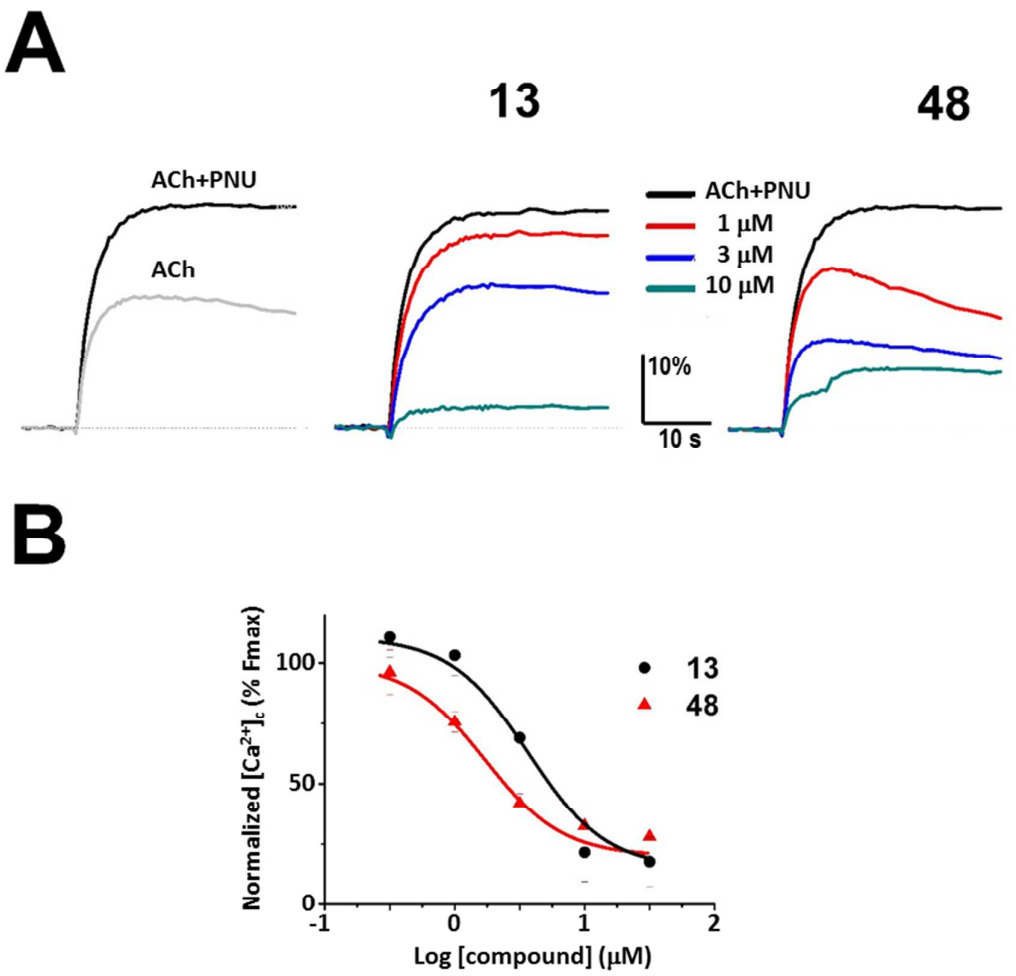

Figure 10. Effects of compounds **13** and **48** on $[Ca^{2+}]_c$ in SH-SY5Y neuroblastoma cells. A) Representative recordings of the increase of $[Ca^{2+}]_c$ induced by the application of 200 µM ACh in the absence and presence of 10 µM PNU120596 (left panel) and the blocking effects of compounds **13** (center panel) and **48** (right panel). Data are represented as % of Fmax-Fmin. B) Normalized concentration-response curves of the inhibitory effects of compounds **13** and **48** on ACh-induced $[Ca^{2+}]_c$ changes. Data have been normalized with respect to the maximal response to ACh plus PNU120596 in the absence of drugs (% Fmax).

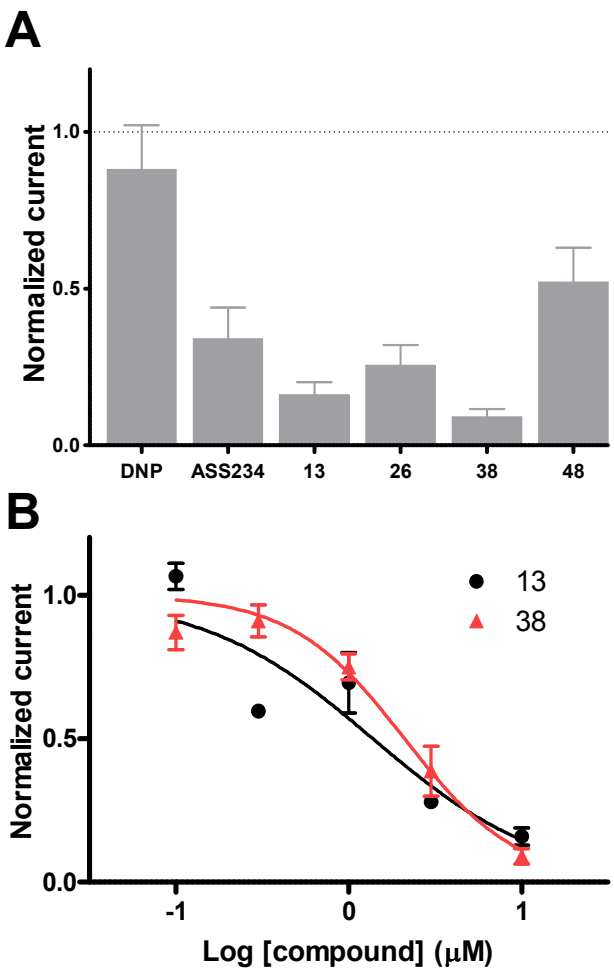

Figure 11. Effects of representative compounds on 5-HT_{3A} receptors. A) Normalized current of 5-HT_{3A} receptors elicited by 3 μM serotonin in the presence of 10 μM of the indicated compounds. B) Dose-response curves of the inhibitory effect of compounds **13** and **38** on peak currents elicited by serotonin in 5-HT_{3A} receptors. Curves are fits to the modified Hill equation with the following parameters (IC_{50} in μM, nH): **13** (1.4 ± 0.4, 0.9 ± 0.2), **38** (2.1 ± 0.3, 1.3 ± 0.2).

Graphical Table of Contents